remote sensing

Article

How to Include Crowd-Sourced Photogrammetry in a Geohazard Observatory—Case Study of the Giant's Causeway Coastal Cliffs

Marion Jaud [1,2,*], Nicolas Le Dantec [1,2], Kieran Parker [3], Kirstin Lemon [3], Sylvain Lendre [4], Christophe Delacourt [1] and Rui C. Gomes [5]

[1] Laboratoire Geo-Oceans—UMR 6538, CNRS, University Brest, Rue Dumont D'Urville, 29280 Plouzané, France; nicolas.ledantec@univ-brest.fr (N.L.D.); christophe.delacourt@univ-brest.fr (C.D.)
[2] IUEM-UMS 3113, CNRS, University Brest, IRD, Rue Dumont D'Urville, 29280 Plouzané, France
[3] British Geological Survey of Northern Ireland, Dundonald House, Upper Newtownards Road, Ballymiscaw, Belfast BT4 3SB, UK; kiepar@bgs.ac.uk (K.P.); klem@bgs.ac.uk (K.L.)
[4] CEREMA, Direction Eau Mer et Fleuves, 134 Rue de Beauvais, 60280 Margny-lès-Compiègne, France; sylvain.lendre@cerema.fr
[5] CERIS, Instituto Superior Técnico, Universidade de Lisboa, Av. Rovisco Pais 1, 1049-001 Lisboa, Portugal; rui.carrilho.gomes@tecnico.ulisboa.pt
* Correspondence: marion.jaud@univ-brest.fr

Abstract: The Causeway Coast World Heritage Site (Northern Ireland) is subject to rockfalls occurring on the coastal cliffs, thus raising major safety concerns given the number of tourists visiting the site. However, such high tourist frequentation makes this site favorable to implement citizen science monitoring programs. Besides allowing for the collection of a larger volume of data, better distributed spatially and temporally, citizen science also increases citizens' awareness—in this case, about risks. Among citizen science approaches, Structure-from-Motion photogrammetry based on crowd-sourced photographs has the advantage of not requiring any particular expertise on the part of the operator who takes photos. Using a mock citizen survey for testing purposes, this study evaluated different methods relying on crowd-sourced photogrammetry to integrate surveys performed by citizens into a landslide monitoring program in Port Ganny (part of the touristic site of the Giant's Causeway). Among the processing scenarios that were tested, the Time-SIFT method allows the use of crowd-sourced data in a very satisfactory way in terms of reconstruction quality, with a standard deviation of 8.6 cm.

Keywords: citizen science; SfM photogrammetry; risk assessment; rockfalls; Time-SIFT method

check for updates

Citation: Jaud, M.; Le Dantec, N.; Parker, K.; Lemon, K.; Lendre, S.; Delacourt, C.; Gomes, R.C. How to Include Crowd-Sourced Photogrammetry in a Geohazard Observatory—Case Study of the Giant's Causeway Coastal Cliffs. *Remote Sens.* **2022**, *14*, 3243. https://doi.org/10.3390/rs14143243

Academic Editor: Joong-Sun Won

Received: 24 May 2022
Accepted: 4 July 2022
Published: 6 July 2022

1. Introduction

Geohazards may lead to damage or risks for human beings or infrastructure. To better understand and anticipate these hazards, it is necessary to know the triggering forcings and precursor signals. This implies regular and distributed monitoring points along the hazard-prone area. In practice, such monitoring can be difficult to implement.

With smartphones, almost all citizens are now equipped with potential sensors and data transmission platforms. Participatory science programs have therefore increased in recent years. Several worldwide support platforms have also been created to support and/or structure citizen science program initiatives. These include, for example, *CitSci* (https://www.citsci.org/ (accessed on 6 December 2021)), *Citizen Science Association* (https://citizenscience.org/ (accessed on 6 December 2021)), *DataONE* (https://www.dataone.org/ (accessed on 6 December 2021)), and *GLOBE* (Global Learning and Observation to Benefit the Environment: https://www.globe.gov/ (accessed on 6 December 2021)).

Citizen science has two major advantages:

(1) Collecting more data that are potentially more frequent or better distributed geographically and therefore make it possible to design a monitoring strategy that is better adapted to the spatial and temporal dynamics of the site.
(2) Increasing awareness of citizens about their environment and contributing to stimulate scientific curiosity. This aspect is particularly interesting for environmental issues and risk prevention, but it is not addressed in the present study.

Nevertheless, in some scientific fields, because of the use of consumer-grade sensors or the low level of expertise of the operators, data collected by citizens always inspire a certain (sometimes justified) distrust. Where citizen data are of lower quality, they can nevertheless be useful, either by providing qualitative information or through quantitative analysis following a different approach from "expert data". Precisely, considering that these citizen data are not analyzed in the same way as expert data, it is up to scientists to develop new processing methods to make the most of these data.

Among the different approaches to citizen science, we can identify, on the one hand, participation in data processing/analysis [1,2], e.g., in data annotation for Deep Learning approaches [3,4], and on the other hand, data collection, which is of particular interest here. For data collection, citizen science has already demonstrated its potential for ecological research, particularly for establishing inventories [5,6]. However, for natural hazards, citizen participation is often limited to reporting and/or dating hazards or hazard markers [7–9].

In general, data from citizen participation have been used mainly in a qualitative way (inventories, reporting, etc. [5–9]), and more rarely in a quantitative way. Moreover, in the case of quantitative analysis of these data, the requirements are generally lower in terms of accuracy, due to the "mainstream" nature of the sensors and the limited expertise of the operators. For example, for the *CoastSnap* beach monitoring system, which was designed to capture the coastline dynamics by using compilations of Smartphone photos [10], the root mean square deviations of shoreline position measurements range from 1.4 to 3.9 m against 0.05 m of accuracy for classical RTK GNSS measurement. Among citizen science approaches, Structure-from-Motion (SfM) photogrammetry based on crowd-sourced photographs has the advantage of relying on observation redundancy during photogrammetric reconstruction and therefore does not require any particular expertise on the part of the operator, as long as the number and distribution of images are adequate [11]. Moreover, the method is relatively flexible in terms of integrating photos acquired with different cameras (even short-focal-length Smartphone cameras) in the same reconstruction [11]. The crowd-sourced photogrammetry method has already been used in archaeology, notably in Cultural Heritage applications [12,13] for digital preservation or reconstruction of lost cultural heritage destroyed either by natural disasters or human-related activities.

Without the addition of external constraints, SfM photogrammetry reconstructions are affected by geometric distortions and/or scaling problems, regardless of the expertise of the operator. Various studies propose solutions to circumvent these distortion problems. The solutions can be grouped into two categories: (i) adding constraints during acquisition or (ii) integrating multi-source data. One commonly used solution is to place ground control points (GCPs) over the area [14–16], but unless there are sufficiently remarkable, fixed points adequately distributed over the study area, this approach is not very applicable to crowd-sourced photogrammetry.

Other solutions include the study by Monkman et al. [17], proposing a methodology to achieve accurate two-dimensional length estimates of fish with an action camera, using a background fiducial marker, a foreground fiducial marker, and a laser marker. In the *CoastSnap* project to map shoreline position, Harley et al. [10] use fixed cradles to constrain the extrinsic parameters of the cameras. RTK GNSS–assisted SfM photogrammetry [18] also relies on knowing some extrinsic parameters of the camera. In an urban context, Hartmann et al. [19] take advantage of the GNSS information (geotag) contained in the EXIF of some crowd-sourced images. Griffiths et al. [13] complete the crowd-sourced photo set by adding photographs with scale bars taken by experts. At last, Wu et al. [20] carried out 3D reconstructions for urban buildings, using crowd-sourced photos supplemented by 2D building vector data for registration.

The touristic site of the Giant's Causeway (Northern Ireland, UK) is subject to certain geohazards, notably rockfalls that put the visitors at risk. Involving visitors in a citizen science program would both raise awareness on the risks and enable the collection of a large number of observations. In this study, we assessed the feasibility and quality of 3D reconstructions for geomorphological monitoring of this natural site, using different crowd-sourced SfM photogrammetry approaches.

2. Methods

2.1. Study Area

The Giant's Causeway and Causeway Coast WHS is located on the north coast of County Antrim in Northern Ireland (Figure 1). It was inscribed on the World Heritage List in 1986 in recognition of its internationally significant geological heritage, but it is also a site of cultural, historical, and touristic significance with tourism at the site dating back more than 300 years. Visitors are attracted by the dynamic coastline of rugged cliffs and 40,000 regularly jointed basalt columns. The primary area for visitors, and the focus of this study, extends 2 km from the Giant's Causeway visitor center, along a developed path at the base of the cliffs leading to what is known as the "Grand Causeway". The path further extends upslope and diverges between the mid slope sections and another that extends to the upper path on the headland. The site is characterized by steep-sided scree slopes that extend from the cliff face to the shoreline.

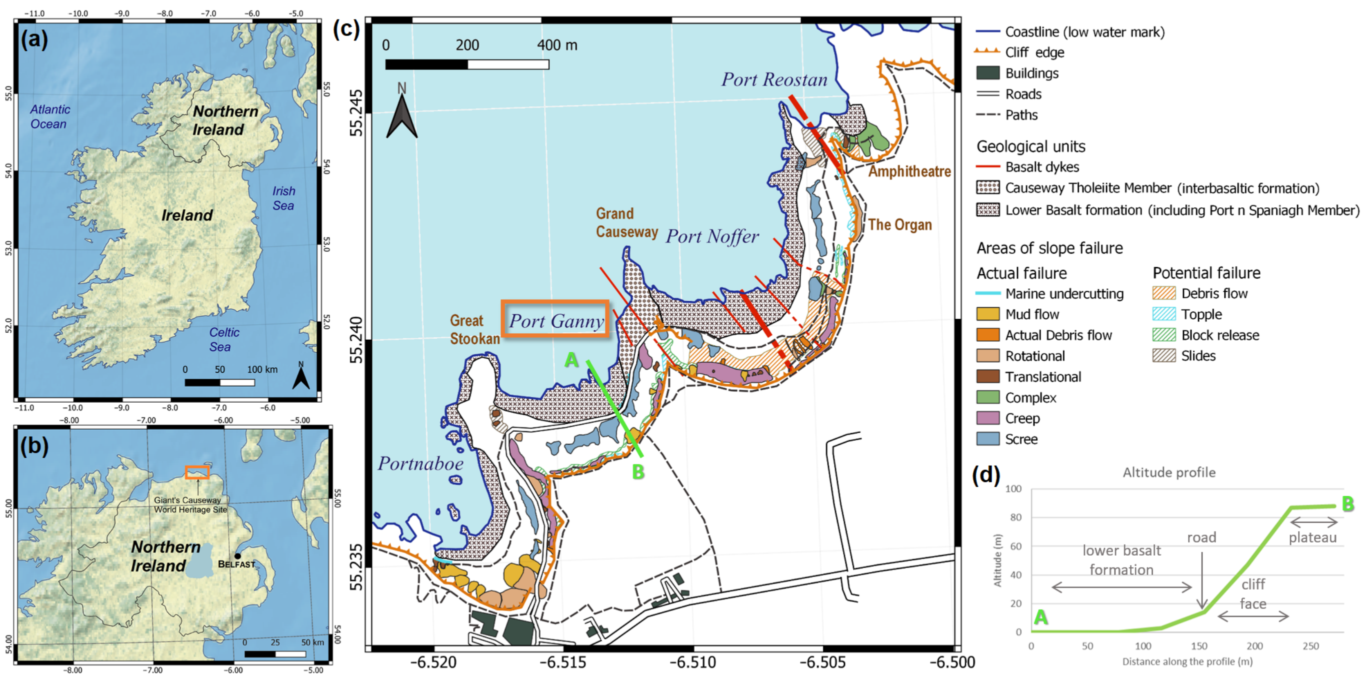

Figure 1. (**a**,**b**) Location of the Causeway Coast and Giant's Causeway in Northern Ireland. (**c**) Map of the Causeway Coast, with geological and geomorphological information, and an identification of actual or potential failure areas (mainly based on Reference [21]). (**d**) Altitude along the AB profile in Port Ganny. This study focuses on surveys carried out in Port Ganny, immediately west of the Grand Causeway (**c**).

2.1.1. Geological Setting

The Giant's Causeway and Causeway Coast WHS are composed of layers of basalt that are part of the Antrim Lava Group. This was formed as a result of extensive volcanism associated with the opening of the North Atlantic Ocean during the Paleogene period, around 60 million years ago. Volcanic activity continued for about 4 million years in three phases separated by two periods of inactivity [22]. The initial phase of volcanic activity created the Lower Basalt Formation (LBF), which was followed by a hiatus. During this time, the uppermost flows of the LBF underwent weathering resulting in sequences of laterite, litghomarge, and bauxite seams known as the Interbasaltic Formation (IBF). Subsidence associated with magma draining led to the formation of a depression creating a deep valley which was then infilled with lava as volcanic activity resumed [23]. The slow cooling of this volume of lava led to the formation of the famous regular columnar-jointed basalts, forming the Causeway Theollite Member (CTM). Another lull in volcanic activity was followed by further lava extrusions, forming the Upper Basalt Formation (UBF). Today the site is characterized by the LBF, weathered horizons of the IBF, and CTM visible on the cliffs, along with high-angled scree slopes.

2.1.2. Site Management

The Giant's Causeway and Causeway Coast WHS is Northern Ireland's premier tourism site, attracting over 1 million visitors every year prior to the COVID-19 pandemic [24]. However, the Giant's Causeway has been attracting visitors since long before it was a tourist attraction and was at the center of a fierce debate disputing the origin of basalt and other igneous rocks in the 18th century. The basalt columns at the Giant's Causeway played a key part in proving that these were, in fact, the product of volcanic activity and, thus, proving the origin of igneous rocks, making it a site of significant importance in the development of geological science [25].

The majority of the site is now under the ownership and management of the National Trust, the UK's largest conservation charity, with 5% remaining in private ownership and the marine elements of the site between the high and low water mark being legally owned by the Crown Estate. A World Heritage Site Steering Group provides the framework for implementing the site's management plan, ensuring that conservation and tourism are carefully balanced. The Steering Group is made up of relevant stakeholders, including the local council, statutory government agencies, the geological survey, universities, and local landowners, ensuring that all interests on the site are taken into consideration.

This site is also one of the five observatory pilots deployed by AGEO (Atlantic Geohazard platform) project, which focuses on Geohazard Risk Management.

2.1.3. Geological Hazards

Geological hazards, in the form of slope failures, combined with increasing visitor numbers and climate change, pose significant challenges to the management of the site.

The area is influenced by regular mass movements in the form of rockfalls, debris slides, complex landslides, and block falls (Figure 2b). Observations over the past two decades have identified that the frequency, intensity, and distribution of slope failures across the site are increasing in response to climatic changes such as increased rainfall and more frequent and prolonged storm events [21]. Over the past decade, the National Trust has recorded over 300 rockfall and landslide events. This poses a potential significant risk to visitors who regularly use the lower coastal paths and also the paths that are developed on the weak scree slope leading to the headland. Much of the slope failures impact the lower path frequently (Figure 1c) used by visitors and The National Trust staff. The natural causes of the slope failure are a combination of the geomorphological steep-sided slopes and cliffs; the variable competency of the geological strata, such as the IBF, which is a weathered horizon; and the undercutting of cliffs by marine erosion. Rainfall plays a major role in triggering slope failure, penetrating the stratigraphy through the jointing within the basalt leading to increased pressure within the slopes and further weathering of the cliff.

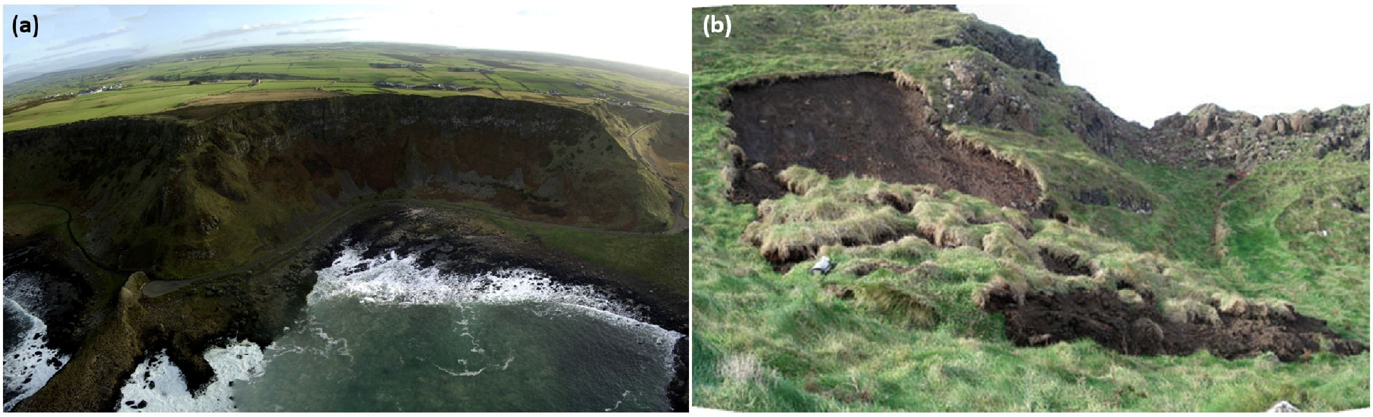

Figure 2. (**a**) Aerial photograph showing Port Ganny. (**b**) Translational slide at Port Ganny, which took place during summer 2008 (photo from Reference [21]).

2.2. Site Monitoring by Terrestrial Photogrammetry

Citizen science monitoring requires consideration of the resources to be used to facilitate the involvement of volunteers and optimize the quality of their measurements. This means, for example, training the volunteers on why and how to participate, developing an application to guide them in their data collection and having an infrastructure that makes it easy to collect and transfer data. Implementing adequate protocols for citizen surveys requires prior knowledge for scientists on data acquisition, processing, and analysis methods, implying a testing phase to account for site-specific constraints. This study corresponds to the stage of "prototyping" of the monitoring method. Although surveys were carried out at Port Noffer and in the Port Reostan amphitheater, this article focuses specifically on the surveys at Port Ganny (Figures 1b and 2a).

2.2.1. "Expert" Reference Dataset

Survey Settings

As the objective is to evaluate the quality of 3D reconstructions integrating crowd-sourced photos, a first survey was carried out on 22 November 2021 in order to constitute an "expert reference dataset" serving as benchmark, which was acquired by using RTK GNSS–assisted SfM photogrammetry [18]. For this survey, a Nikon D800 reflex camera (20 mm focal length, Nikon, Tokyo, Japan) was used (Figure 3a). A total of 544 photos were collected, including 204 georeferenced photos from 8 stations with GNSS RTK positioning of the camera (Figure 3b). The resolution is, on average, 2.2 cm/pixel. The GNSS antenna was a Leica 1200+ device (Leica Geosystems, Aarau, Switzerland).

It is conceivable that such monitoring could be carried out by trained site-management staff.

Data Processing

The acquired photos were processed by SfM photogrammetry, using *Agisoft Metashape*® (Agisoft LLC., St. Petersburg, Russia), according to the following processing chain (Figure 4a) [18]:

- Creation and formatting of a camera position file compatible with *Agisoft Metashape*®;
- Image orientation by bundle adjustment (detection and matching of homologous key points in overlapping photographs). This step allows us to compute the extrinsic parameters of each camera.
- Refinement of camera calibration parameters (intrinsic parameters) by optimization, using the redundancy of information on pixels observed in several images and the RTK-georeferenced camera positions. The RTK GNSS–measured positions are taken as initial values, and their variations are constrained here in a radius of 10 cm.
- Dense image matching to produce a dense point cloud by using the estimated extrinsic and intrinsic camera parameters.

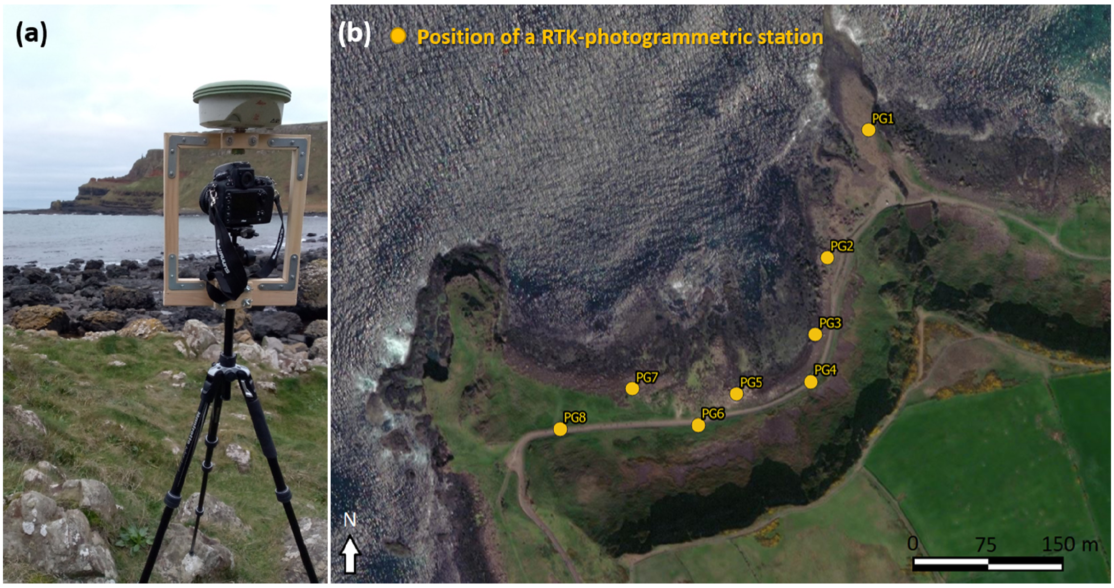

Figure 3. (**a**) Measurement system developed for the Real-Time Kinematic (RTK) Global Navigation Satellite System (GNSS)–assisted terrestrial Structure-from-Motion (SfM) photogrammetry method (equipped here with the Nikon D800 Reflex camera and the Leica 1200+ GNSS antenna). (**b**) Positions of the measured camera stations for the RTK GNSS–assisted photogrammetric survey (PG: Port Ganny stations).

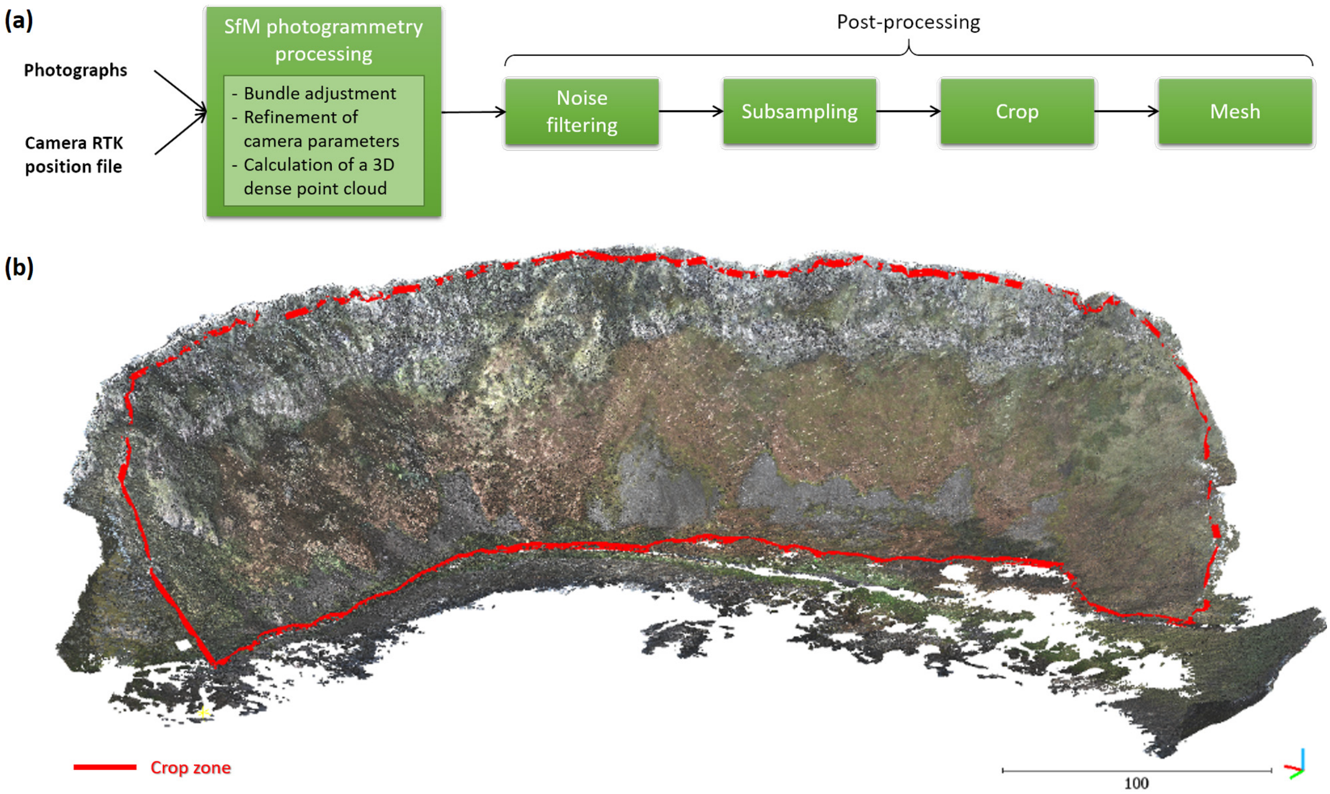

Figure 4. (**a**) Processing chain for the "expert" dataset used as reference. The SfM photogrammetry processing is performed by using *Agisoft Metashape*, and postprocessing steps are performed by using *CloudCompare*. (**b**) Resulting 3D mesh before cropping to a common zone for comparison.

With such a method, the reconstruction accuracy is within 5 cm (or lower). The dense point cloud (about 65 $\times$ 10^6 points) is exported to the open-source software *CloudCompare*® (CloudCompare open project, EDF R&D, Paris, France). The point cloud is then filtered with the SOR (Statistical Outlier Removal) filter proposed by *CloudCompare*®. It is then subsampled to 3 cm in order to keep the computation time manageable for the next steps of this study. To limit edge effects, a common comparison zone is defined (Figure 4b), and the point cloud is cropped according to this zone and finally meshed. This mesh will be used as a reference model to assess the quality of reconstructions by using crowd-sourced pictures.

Such a survey is carried out in a few hours and can be operated by the site managers. The duration of data processing can vary from a few hours to a few days for processing depending on the power of the computer used (here, it lasted 2 h, using an Intel(R) HD Graphics 630).

2.2.2. Use of Crowd-Sourced Images

Survey Settings

For this study, the volunteer group was composed of academics (a majority of whom were not familiar with photogrammetry methods). Once the areas of interest were defined, volunteers were asked to take photos (if possible geotagged, without zoom, and in landscape mode) with their smartphones. These acquisitions were spread over two days (22 November 2021 and 25 November 2021) and at different times of the day. Seven different smartphone models were used and are described in Table 1. More than 700 photos were acquired by the volunteer group.

Table 1. Smartphone devices used during the simulation of crowd-sourced acquisition.

Devices	Focal Length (mm)	Image Size
CrossCall Core-X4 (Croscall, Aix-en-Provence, France)	4.71	4000 × 3000
Wiko Y80 V680 (Wiko SAS, Marseille, France)	3.6	4096 × 2304
Huawei POT-LX1 (Huawei Technologies Co., Ltd., Shenzhen, China)	3.6	4160 × 3120
Samsung SM-A125 (Samsung electronics, Seoul, Korea)	4.6	4000 × 3000
Samsung SM-A127 (Samsung electronics, Seoul, Korea)	5.0	4000 × 3000
iPhone XR (Apple, Cupertino (Californie), USA)	4.25	4032 × 3024
iPhone 5s (Apple, Cupertino (Californie), USA)	4.0	3264 × 2448

To make the acquisition more realistic, some “inadequate” photos were collected: pictures outside of the area of interest, blurred images, selfies, photos of people, photos taken unintentionally, etc. In addition, despite the instructions, some photos were acquired without geotag (24%), or with a zoom or in portrait mode (4.9%). Among these non-optimal images, only the photos outside the area of interest are removed (for this pre-filtering step, the geotag can help if it is present), leaving a total of 684 smartphone photos used in the tests described below.

Data Processing at a Given Date

Different processing scenarios are proposed to exploit these crowd-sourced images, some of which also use images from the reference survey (544 photos acquired with the Nikon D800 reflex camera). The first series of scenarios (Tests 1 to 5) aims to reconstruct the entire area, while minimizing the proportion of RTK georeferenced images from the reference survey that need to be included. These different processing scenarios are as follows (Table 2):

- Test 1: The dataset consists of a subset of the reference dataset, including some georeferenced and all non-georeferenced photos. The number of RTK stations is limited here to 5 (PG1, PG2, PG4, PG5, and PG8 stations on Figure 3b).
- Test 2: The dataset is composed of the georeferenced Nikon camera photos acquired from the same 5 RTK stations of Test 1 and all the smartphone photos acquired with the 7 different cameras, both from the foot of the cliff and from the top of the cliff.
- Test 3: The dataset is once again composed of the georeferenced Nikon-camera photos acquired from the same 5 RTK stations of Test 1 and all the photos acquired with the 7 smartphone cameras, but applying a filter on the smartphone photos after the "Bundle adjustment" step. With this filter, we deactivated the photos whose alignment error was greater than twice the standard deviation and re-ran the SfM processing chain.
- Test 4: For this scenario, only Smartphone photographs are used. All 684 smartphone photos are used, whether geotagged or not, acquired on different dates (22 November 2021 and 25 November 2021) or acquired from the cliff foot or the cliff top.
- Test 5: The dataset is, again, composed only of smartphone photographs, geotagged or not, acquired at different dates, but only those acquired from the cliff foot (the cliff top being potentially dangerous for citizens).

Table 2. Sets of photographs used in each processing scenario.

Processing Scenario	Sets of Photographs Used
Expert reference dataset	Georeferenced Nikon D800 photographs (from 8 georeferenced stations) + non-georeferenced Nikon D800 photographs
Test 1	Georeferenced Nikon D800 photographs (from 5 georeferenced stations) + non-georeferenced Nikon D800 photographs
Test 2	Georeferenced Nikon D800 photographs (from 5 georeferenced stations) + all smartphone photographs
Test 3	Georeferenced Nikon D800 photographs (from 5 georeferenced stations) + smartphone photographs filtered by alignment quality after bundle adjustment
Test 4	All smartphone photographs
Test 5	Smartphone photographs collected from cliff foot
Test 6 (Time-SIFT method)	Smartphone photographs at t1 + dataset of reference at t0 for bundle adjustment step (here, georeferenced Nikon D800 photographs from 5 georeferenced stations)

For each of these 5 test scenarios, the processing chain is the same (Figure 5a), i.e., SfM photogrammetry processing in *Agisoft Metashape* (similar to that described above) and postprocessing in *CloudCompare*. The postprocessing consists of registering the point cloud with the reference mesh (using the "Iterative Closest Point" method). The point cloud is then cleaned, first manually, when necessary; then automatically, using the SOR filter; and then subsampled to 3 cm and cropped to the same area as the reference cloud. Finally, the point cloud is compared to the reference mesh by calculating distances for all points in the cloud with a cloud-to-mesh approach.

Data Processing Using the Time-SIFT Method

In the framework of an observatory, one can take advantage of the multi-date aspect of the datasets, using the Time-SIFT approach for the processing of crowd-sourced data. The Time-SIFT method, proposed by Feurer and Vinatier [26], is based on the properties of the SIFT (Scale Invariant Feature Transform) algorithm used for image alignment in SfM processing [27]. This Time-SIFT method consists of performing the bundle adjustment step (to determine the extrinsic and intrinsic parameters of the cameras) by using the largest possible set of photos, which are then separated into several groups for the computation of the dense point cloud. The images of the different groups can correspond to photo sets acquired at different dates, as long as a part of the imaged area remains invariant and recognizable between these different groups. With this method, it is therefore possible to consider "camera groups" containing fewer images and with less overlap, the density of information necessary for the correct estimation of camera models being provided by the superposition of the different groups.

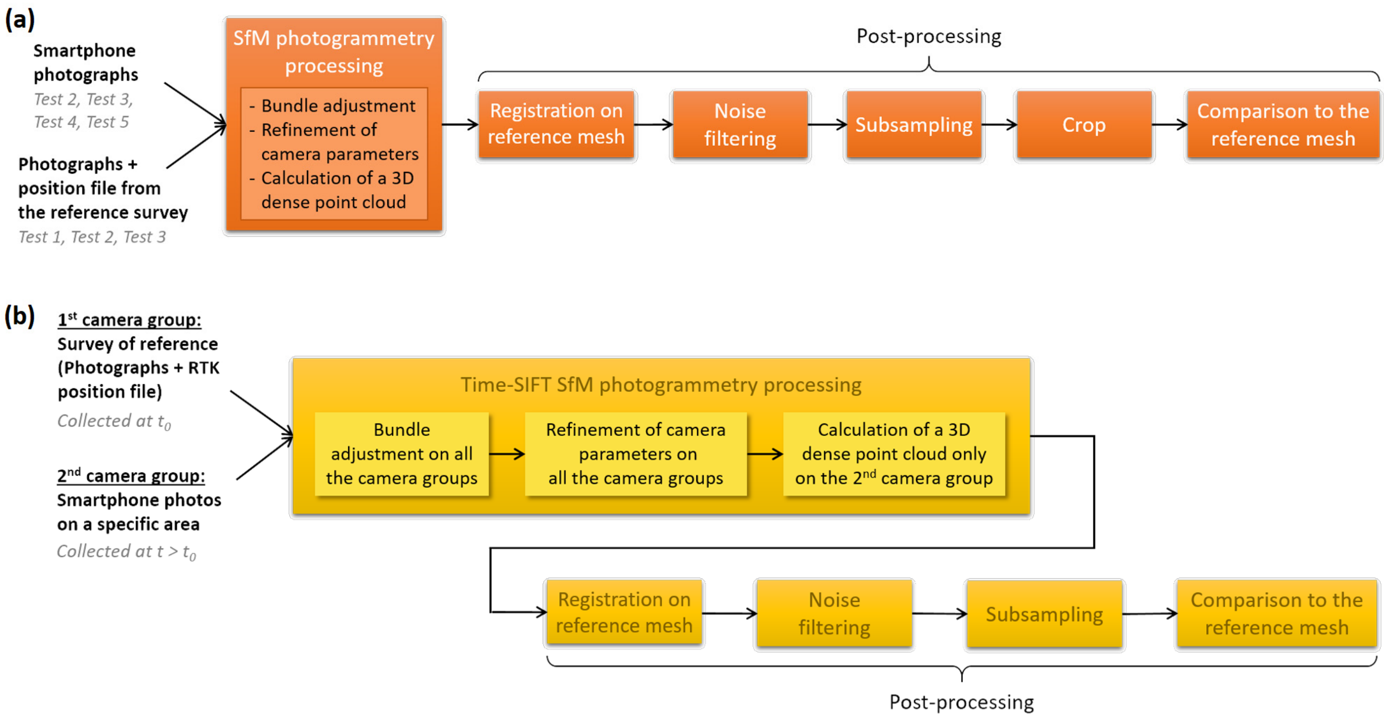

Figure 5. (**a**) Processing chain with «classical» SfM photogrammetry and postprocessing in CloudCompare used for Tests 1 to 5. (**b**) Processing chain with Time-SIFT SfM processing and postprocessing in CloudCompare used for Test 6.

This approach therefore presents a great potential for crowd-sourced photogrammetry. Indeed, it seems unrealistic to expect that crowd-sourced photographs will perfectly cover the whole area with sufficient overlap. Using the Time-SIFT method, it would be possible to focus on "hotspot areas", working on smaller groups of photos. During bundle adjustment, these small groups of photos can be aligned with a reference dataset collected with the RTK GNSS–SfM photogrammetric approach, even if it has not been acquired at the same date (as long as part of the area remains invariant). Thus, another processing scenario was set up:

- Test 6: For this test, we are working on a focused area (the screes SW of Port Ganny; see Figure 4b). The aim is to reconstruct this area by using 330 smartphone photos, geotagged or not, collected from the foot of the cliff on 25 November 2021. For processing in Time-SIFT mode (Figure 5b), these smartphone photos are aligned, during the bundle adjustment, with 205 additional photos acquired on 22 November 2021, using the Nikon D800 camera with RTK georeferencing.

3. Results

As long as the geometric reliability of the RTK stations network is maintained (stations spanning a sufficiently large part of the studied area and non-alignment of the stations to avoid georeferencing ambiguities), the decrease from eight to five RTK stations (Test 1) has only a very moderate impact on the quality of the reconstruction. Indeed, when comparing the dense point cloud with the reference mesh, we obtained a mean error of −0.5 cm and a standard deviation of 4.6 cm (Table 3).

Table 3. Cloud-to-mesh distances between the mesh resulting from the "expert dataset" (used as reference) and the different scenarios testing the incorporation of crowd-sourced photographs.

	Test 1	Test 2	Test 3	Test 4	Test 5	Test 6
Mean error	−0.5 cm	−0.8 cm	0.2 cm	1.7 cm	1.2 cm	0.0 cm
Std. deviation	4.6 cm	32.1 cm	16.9 cm	3.92 m	2.06 m	8.6 cm

The use of photos from different sensors (here, Nikon SLR camera and the seven smartphones tested—Table 1) implies different camera settings in terms of sensitivity, exposure, saturation, etc. This diversity of sensors, combined with variable illumination conditions, makes the detection of tie-points and, therefore, the image-matching stage more complicated. This contributes to the appearance of "ghost structures" on the raw point clouds (Figure 6), which are pseudo-coherent but aberrantly placed reconstructions due to "sub-networks" of cameras that have not been connected to the main camera network [19]. These ghosting effects are most pronounced in Tests 2 and 4 (i.e., those involving shots from the cliff top, hence where the survey configuration favors the appearance of a separate camera network). To a lesser extent, some limited ghosting effects appeared in Tests 5 and 6. In all cases, these ghost structures are removed manually.

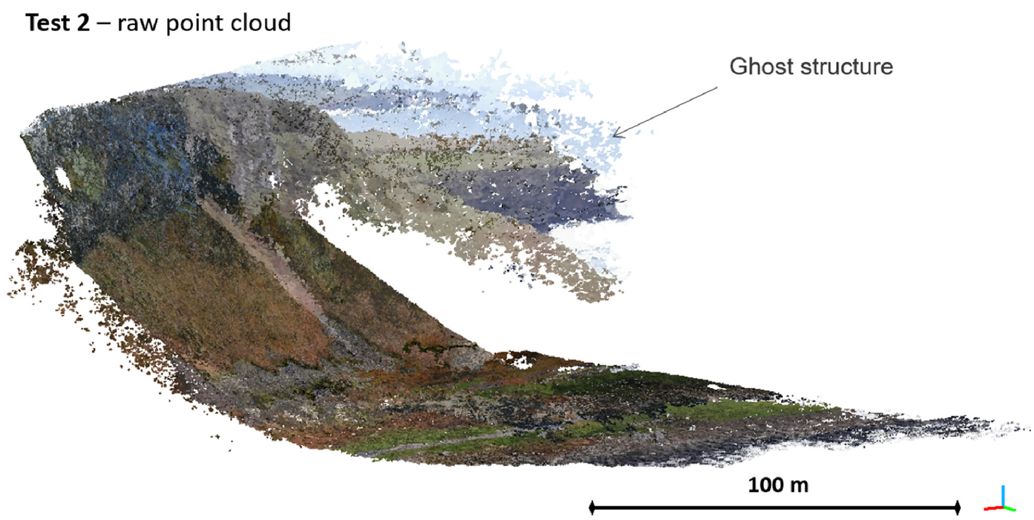

Figure 6. Example of «ghosting effect» on the raw dense point cloud generated by Agisoft Metashape for Test 2.

The comparison of Tests 2, 3, 4, and 5 shows that the addition of photos from a SfM RTK photogrammetry survey to the crowd-sourced photographs greatly improves (about ten times better) the quality of the reconstruction (Table 3). Indeed, the standard deviations of Tests 2 and 3 (with georeferenced photos from the reference survey) are, respectively, 32.1 cm and 16.9 cm, against 3.92 m and 2.06 m for Tests 4 and 5 (only with smartphone photos). Moreover, in both cases, preselecting the images, either according to their alignment error (Test 3) or simply according to the relevance of the point of view (here, for example, the foot of the cliff in Test 5), also makes it possible to improve the accuracy (about twice as good) of the reconstruction compared to processing without preselection (Tests 2 and 4, respectively).

With the Time-SIFT method (Test 6), including reference survey photos (here, georeferenced Nikon D800 photographs) in the alignment step and then reconstructing the dense point cloud only from the crowd-sourced data increases the consistency of each camera group without reducing the constraints on the estimation of camera parameters. This approach allows the use of crowd-sourced data in a very satisfactory way in terms of reconstruction quality, since the standard deviation is 8.6 cm.

Figures 7 and 8 show the spatial distribution of errors. It can be seen that error zones or non-reconstructed zones are often present in the lower part of the area. This can be explained by the low angle at which the photographs are taken in relation to the imaged surface (which is a source of uncertainty in the reconstruction), where the topography starts to flatten. In addition, it also corresponds to areas with taller vegetation (bushes and ferns), which makes the photogrammetric reconstruction complicated, especially in windy conditions. An error zone is also often present at the top right of the area, possibly due to the presence of small shrubs causing noisier reconstructions.

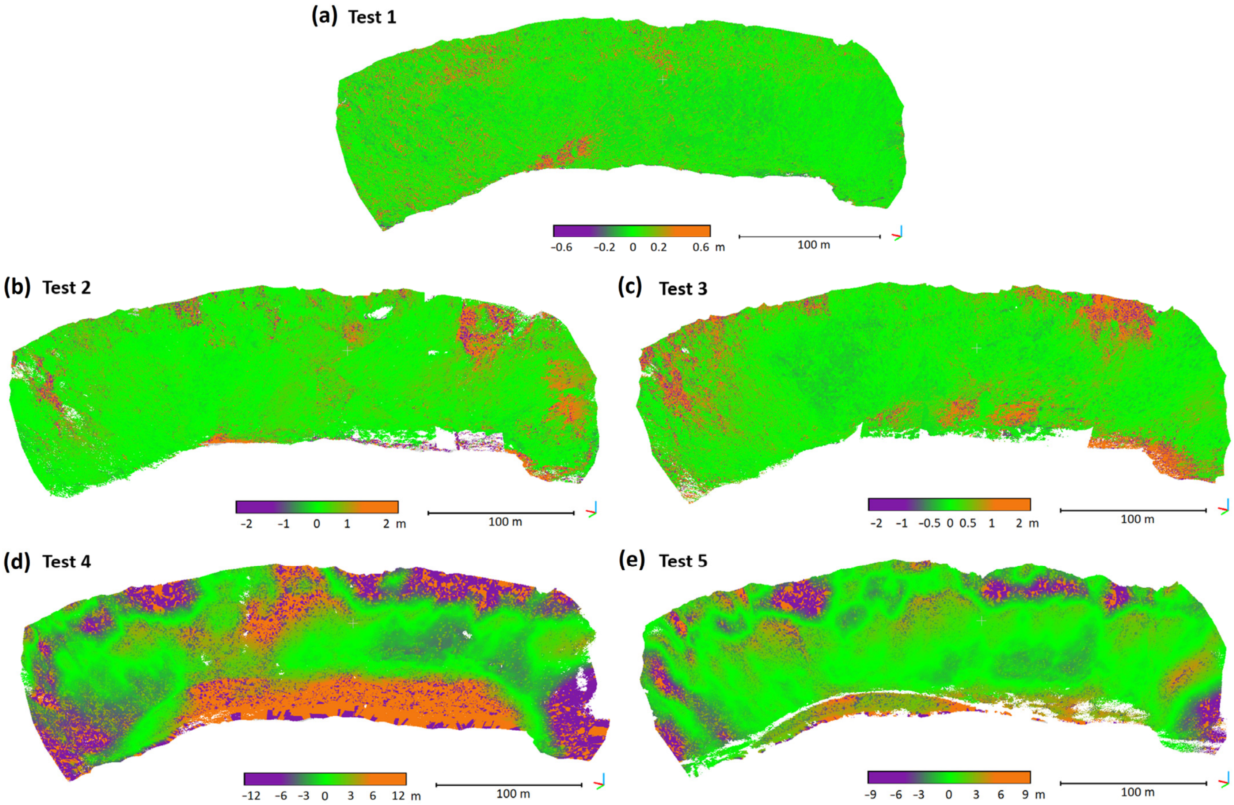

Figure 7. Spatial distribution of the cloud-to-mesh distances between the mesh resulting from the "expert dataset" (used as reference) and the different scenarios testing the incorporation of crowd-sourced photographs (illustrations (**a**–**e**) corresponding, respectively, to Tests 1 to 5). Note: The color scale varies between the different tests.

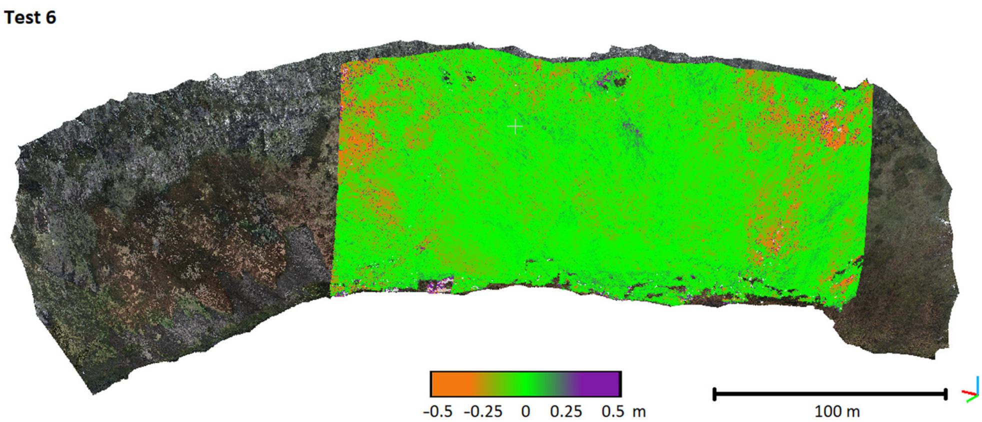

Figure 8. Spatial distribution of the cloud-to-mesh distances between the mesh resulting from the "expert dataset" (used as reference) and the point cloud corresponding to the area reconstructed by using Time-SIFT SfM photogrammetry.

4. Discussion

4.1. Data Quality in Citizen Science

As citizens may lack scientific expertise or technical skills, citizen data quality is widely discussed in the literature (see, for example, References [28–30]). Nevertheless, some studies show that a variety of citizen science projects have produced data with quality equal to or higher than the dataset collected by professionals [29].

It depends on what is meant by "quality" (accuracy of the measurement, distribution of measurements, sufficient sample size, etc.). In this case of geomorphological monitoring, the quality threshold depends on the amplitude of the signal to be detected. Here, we are interested in landslides or rockfalls corresponding to distance between pre- and post-event surfaces in the order of 10 cm to 10 m.

The residual errors after registration with the reference reconstruction (measured here by the standard deviation) correspond to distortion or reconstruction problems (for large errors of the order of several meters) or noise (for errors of a few centimeters to a few tens of centimeters). As mentioned in Reference [31], the high standard of quality that is achieved quickly, simply, and at a low cost by using crowd-sourced photogrammetry combined with the Time-SIFT method is more than suitable for characterizing most geohazards.

One of the advantages of crowd-sourced photogrammetry is that, from the citizen's point of view, it is a participatory science activity without protocol. This is particularly interesting when working with tourists, who typically, at least for non-national visitors, only come to the site once, so that one cannot expect them to participate if they need to be familiar with a complex protocol. Here, as everyone knows how to take a picture, the only criterion to be considered is the relevance of the photographed area. As long as the area of interest is visible in enough images and from enough distinct points of view (the more participants there are, the easier these criteria are fulfilled), the dataset is not affected by the scientific or technical skills of the "operators". Indeed, the quality of the 3D reconstruction depends mainly on the processing strategy.

Moreover, in the case of a very large number of participants, in order to limit processing times, it is possible to pre-filter the photos according to their relevance, for example, by removing redundant photos on the over-photographed areas.

4.2. Technical Suggestions for Improving the Method

In practice, limiting the number of RTK stations enables reducing the survey time for site management staff. Alternatively, fixed pivoting stations could be set up to serve as Smartphone supports, which would make it possible to do without the RTK GNSS–assisted SfM photogrammetry frame and tripod.

In order to limit the ghosting effects, it might be possible to develop a routine to equalize the colorimetry of the images beforehand. Since the photos transferred by citizens are generally in JPEG format, care should be taken to ensure that these manipulations do not affect the quality of the images and interfere with the SfM photogrammetry reconstruction.

One of the important points for the implementation of a long-term monitoring program by using crowd-sourced photogrammetry is to determine the frequency of SfM RTK photogrammetry reference surveys, as well as the relevant frequency to group the crowd-sourced images for the Time-SIFT processing method. These criteria depend both on the rate of morphological evolution (the frequency of occurrence of mass movements induced by the major hazards (rockfalls, landslides, etc.) and on the seasonal evolution of the site (e.g., evolution of the color and size of the vegetation). In the event of a major change in the morphology of the site, it is recommended that a new reference survey be carried out. Time-SIFT photo groups should be set up in such a way that the imaged areas are morphologically stable over the period of acquisition of photos within each group and that the images in the same group have a consistent appearance (e.g., no morphological evolution or color change within the same group).

The development of a smartphone app dedicated to the acquisition of these crowd-sourced photos would make it possible to better constrain certain image acquisition recommendations, e.g., take photos in landscape mode to maximize coverage and not have to deal with different orientations, prevent zooming, ensure that the images have a geotag, etc. This application could also allow citizens to transfer their photographs more easily, either via a 4G connection, free Wi-Fi hotspot, or via Bluetooth to a terminal dedicated for data collection that would be installed on the site, for instance, near the visitor center. With geotagged images, the app could even use citizen photographs that have already been acquired to create heat maps of photographed areas and guide citizens in choosing which areas to photograph while they are taking photographs. The creation of heat maps of photographed areas could also help to identify over-photographed areas, which is where some photos could be removed at the stage of data processing to reduce processing times.

4.3. Interactions with Citizens

Involving citizens in a photogrammetric survey requires thinking of a way to give some explanations beforehand: Why is it important to monitor this site? What will the data collected be used for? What is the best way to collect the data? Apart from using a smartphone app, on a tourist site such as the Giant's Causeway, there are several ways of informing potential participants: explanatory panels at the visitor center or at the entrance to the site, information on audio guides, information directly transmitted via the site management staff, etc. In particular, citizens must be made aware of the fact that they should not put themselves in danger in order to collect images (by approaching a cliff edge or a rockfall, for example). The results of the project could also be advertised through a website, at the visitor center with virtual exhibitions, or through the mobile app, using Augmented Reality, as it has been performed in the HeritageTogether project [32]

Although many studies (e.g., Reference [33]) point out the long-term commitment of citizens as a major challenge, working on a tourist site is an asset. Indeed, as the target audience mainly consists of tourists, the question of maintaining citizen engagement is not so critical. Nevertheless, citizens are more likely to participate if they receive feedback. Here, the information regarding the monitoring program that would be provided at an exhibit in the visitor center or on a dedicated app or website could also show prior results, using participatory data.

While adding the photographs to a heat map as the images are transferred would use computing resources (the cost-benefit ratio would need to be assessed by also considering the associated carbon footprint), using the geotag information to overlay on a map the locations from which the pictures were taken is more straightforward. In order to further promote citizen participation and even to guide citizens, the image acquisition could be thought of as a playful activity, such as *Pokemon Go* (https://pokemongolive.com/en/ (accessed on 16 March 2022)).

4.4. Integration of These Results into an Observatory Strategy

The opportunity of monitoring the 3D morphological evolutions over time is an asset for the management of the site. Indeed, in addition to the volume balances and the more precise assessment of erosion rates and their variability in space and in time, the time series of 3D reconstructions also allows a more complete vision (notably spatially) of the hazard markers and thus a better understanding of the processes at play. It is possible to integrate these data into a multi-source monitoring approach by coupling them with geotechnical and hydrological measurements, for example, in order to have a more complete panel of measured variables and thus a better anticipation of events.

To complement these surveys and better identify the dates of hazards (and thus the relevant periods for processing crowd-sourced data), video monitoring could be considered. Indeed, even if they do not allow us to produce 3D models, surveillance cameras are widely used to better constrain the temporal component of environmental observations, with low costs and human efforts (see References [34–36]). However, it implies that a system (video sensor, data supply, and transfer modes) that is compatible with the site constraints should be designed. Their use also requires the identification of a suitable location (viewpoint and distance from the monitored area), which also needs to be non-disruptive in this preserved area.

In the framework of a geo-hazard observatory and of a long-term monitoring strategy, in order to convey the results derived from this citizen science dataset in a way that can be understood by all the stakeholders involved in management (including the citizens potentially contributing to the acquisition of photographs), hazard "indicators" can be defined to serve both as evaluation and decision-making tools. These indicators are a simplified representation of the measured variables, according to a postprocessing method typically involving formulae combining several variables, spatial interpolation, and discretization into classes. Since the use of indicators implies a certain "smoothing" of the measurement results, there is a higher tolerance to measurement errors, which is well-suited for crowd-sourced photogrammetric monitoring. In order to better reflect the sensitivity of the data (the capacity to detect and discriminate mass movements of different types, at different scales, and related to different processes), indicators can be derived on a high-resolution grid since SfM photogrammetry provides dense point clouds.

5. Conclusions

The Giant's Causeway is a very attractive site for tourists, but the cliffs bordering the site present a significant risk of mass movements and falling rocks. The site is therefore subject to extensive surveillance by the stakeholders. Given that implementing in situ instruments on such a site is complicated, it appears interesting to combine in a crowd-sourced photogrammetry approach the possibilities of in situ remote sensing methods and the opportunity of the number of potential operators considering all the visitors. Furthermore, the involvement of citizens through a participatory science program appears to be a real opportunity to educate them about geohazards and, more broadly, about the observation of the environment.

The tests demonstrate that combining crowd-sourced photographs and the Time-SIFT processing approach (based on expert surveys) allows us to provide 3D reconstructions with precision within 10 cm (here a standard deviation of 8.6 cm). Although some practical implementation issues remain to be resolved, complementing reference RTK GNSS–assisted terrestrial SfM photogrammetry surveys with crowd-sourced photogrammetry surveys offers a great potential. Indeed, it becomes possible to space out the reference surveys while collecting, thanks to citizens, more frequent measurements that are better distributed in time, and therefore allowing better dating of events or changes. Thus, it will be easier to target the link between the event and the triggering processes to improve the understanding of the mechanisms and thus improve the anticipation of hazards.

Author Contributions: Conceptualization, M.J.; methodology, M.J.; software, M.J.; validation, M.J. and N.L.D.; formal analysis, M.J.; investigation, M.J., N.L.D., K.P., K.L. and S.L.; resources, M.J., N.L.D. and K.P.; data curation, M.J.; writing—original draft preparation, M.J., N.L.D., K.P., K.L. and S.L.; writing—review and editing, M.J. and N.L.D.; visualization, M.J.; supervision, R.C.G. and C.D.; project administration, R.C.G., N.L.D., K.P. and K.L.; funding acquisition, R.C.G. and C.D. All authors have read and agreed to the published version of the manuscript.

Funding: This research received no external funding.

Data Availability Statement: The reference dataset (3D point cloud) is available on the Indigéo portal: https://doi.org/10.35110/2774795b-e223-47c7-82d4-03f2b2ceecef.

Acknowledgments: The authors acknowledge financial support provided by the European program Interreg Atlantic Area via the project AGEO (EAPA 884/2018). The authors would also like to thank the National Trust for providing access to the sites.

Conflicts of Interest: The authors declare no conflict of interest.

References

1. Simpson, R.; Page, K.R.; De Roure, D. Zooniverse: Observing the world's largest citizen science platform. In Proceedings of the 23rd International Conference on World Wide Web, ACM, Seoul, Korea, 7–11 April 2014. [CrossRef]
2. Stewart, C.; Labrèche, G.; González, D.L. A Pilot Study on Remote Sensing and Citizen Science for Archaeological Prospection. *Remote Sens.* **2020**, *12*, 2795. [CrossRef]
3. Langenkämper, D.; Simon-Lledó, E.; Hosking, B.; Jones, D.O.B.; Nattkemper, T.W. On the impact of Citizen Science-derived data quality on deep learning based classification in marine images. *PLoS ONE* **2019**, *14*, e0218086. [CrossRef]
4. Papakonstantinou, A.; Batsaris, M.; Spondylidis, S.; Topouzelis, K. A Citizen Science Unmanned Aerial System Data Acquisition Protocol and Deep Learning Techniques for the Automatic Detection and Mapping of Marine Litter Concentrations in the Coastal Zone. *Drones* **2021**, *5*, 6. [CrossRef]
5. Dickinson, J.L.; Shirk, J.; Bonter, D.; Bonney, R.; Crain, R.L.; Martin, J.; Phillips, T.; Purcell, K. The current state of citizen science as a tool for ecological research and public engagement. *Front. Ecol. Evol.* **2012**, *10*, 291–297. [CrossRef]
6. Joly, A.; Bonnet, P.; Goëau, H.; Barbe, J.; Selmi, S.; Champ, J.; Dufour-Kowalski, S.; Affouard, A.; Carré, J.; Molino, J.-F.; et al. A look inside the Pl@ntNet experience: The good, the bias and the hope. *Multimed. Syst.* **2016**, *22*, 751–766. [CrossRef]
7. Bond, C.E.; Howell, J.; Butler, R. Public engagement in 3D flood modelling through integrating crowd sourced imagery with UAV photogrammetry to create a 3D flood hydrograph. In Proceedings of the AGU Fall Meeting, San Francisco, CA, USA, 12–16 December 2016.
8. Boger, R.; Low, R.; Nelson, P. Identifying Hurricane Impacts on Barbuda Using Citizen Science Ground Observations, Drone Photography and Satellite Imagery. *Int. Arch. Photogramm. Remote Sens. Spatial Inf. Sci.* **2020**, *XLII-3/W11*, 23–28. [CrossRef]
9. Kocaman, S.; Gokceoglu, C. Possible Contributions of citizen science for landslide hazard assessment. *Int. Arch. Photogramm. Remote Sens. Spatial Inf. Sci.* **2018**, *XLII-3/W4*, 295–300. [CrossRef]
10. Harley, M.D.; Kinsela, M.A.; Sánchez-García, E.; Vos, K. Shoreline change mapping using crowd-sourced smartphone images. *Coast. Eng.* **2019**, *150*, 175–189. [CrossRef]
11. Jaud, M.; Kervot, M.; Delacourt, C.; Bertin, S. Potential of Smartphone SfM Photogrammetry to Measure Coastal Morphodynamics. *Remote Sens.* **2019**, *11*, 2242. [CrossRef]
12. Vincent, M.L.; Gutierrez, M.F.; Coughenour, C.; Manuel, V.; Bendicho, L.-M.; Remondino, F.; Fritsch, D. Crowd-sourcing the 3D digital reconstructions of lost cultural heritage. In Proceedings of the Digital Heritage IEEE Conference, Granada, Spain, 28 September–2 October 2015. [CrossRef]
13. Griffiths, S.; Edwards, B.; Wilson, A.; Karl, R.; Labrosse, F.; LaTrobe-Bateman, E.; Miles, H.; Moeller, K.; Roberts, J.; Tiddeman, B. Small Works, Big Stories—Methodological approaches to photogrammetry through crowd-sourcing experiences. *Internet Archaeol.* **2015**, *40*. [CrossRef]
14. James, M.R.; Robson, S. Straightforward reconstruction of 3D surfaces and topography with a camera: Accuracy and geoscience application. *J. Geophys. Res.* **2012**, *117*, F03017. [CrossRef]
15. Tonkin, T.; Midgley, N. Ground-Control Networks for Image Based Surface Reconstruction: An Investigation of Optimum Survey Designs Using UAV Derived Imagery and Structure-from-Motion Photogrammetry. *Remote Sens.* **2016**, *8*, 786. [CrossRef]
16. Jaud, M.; Passot, S.; Allemand, P.; Le Dantec, N.; Grandjean, P.; Delacourt, C. Suggestions to Limit Geometric Distortions in the Reconstruction of Linear Coastal Landforms by SfM Photogrammetry with PhotoScan® and MicMac® for UAV Surveys with Restricted GCPs Pattern. *Drones* **2019**, *3*, 2. [CrossRef]
17. Monkman, G.G.; Hyder, K.; Kaiser, M.J.; Vidal, F.P. Accurate estimation of fish length in single camera photogrammetry with a fiducial marker. *ICES J. Mar. Sci.* **2020**, *77*, 2245–2254. [CrossRef]
18. Jaud, M.; Bertin, S.; Beauverger, M.; Augereau, E.; Delacourt, C. RTK GNSS-Assisted Terrestrial SfM Photogrammetry without GCP: Application to Coastal Morphodynamics Monitoring. *Remote Sens.* **2020**, *12*, 1889. [CrossRef]
19. Hartmann, W.; Havlena, M.; Schindler, K. Towards complete, geo-referenced 3D models from crowd-sourced amateur images. *ISPRS Ann. Photogramm. Remote Sens. Spat. Inf. Sci.* **2016**, *III–3*, 51–58. [CrossRef]
20. Wu, J.; Mao, J.; Chen, S.; Zhuoma, G.; Cheng, L.; Zhang, R. Building Facade Reconstruction Using Crowd- Sourced Photos and Two-Dimensional Maps. *Photogramm. Eng. Remote Sens.* **2020**, *86*, 677–694. [CrossRef]
21. Smith, B.J.; Pellitero Ondicol, R.; Alexander, G. Mapping Slope Instability at the Giant's Causeway and Causeway Coast World Heritage Site: Implications for Site Management. *Geoheritage* **2011**, *3*, 253–266. [CrossRef]
22. Mitchell, W. *The Geology of Northern Ireland: Our Natural Foundation*, 1st ed.; Geological Survey of Northern Ireland: Belfast, Northern Ireland, 2004.
23. Simms, M.J. Subsidence, not erosion: Revisiting the emplacement environment of the Giant's Causeway, Northern Ireland. *Proc. Geol. Assoc.* **2021**, *132*, 537–548. [CrossRef]
24. NISRA. Northern Ireland Visitor Attraction 2019 Survey Report. 2020. Available online: https://www.nisra.gov.uk/sites/nisra.gov.uk/files/publications/NI-tourism-publication-Visitor-Attraction-Survey-2019-Report.pdf (accessed on 9 March 2022).
25. Higgs, B.; Wyse-Jackson, P.N. The role of women in the history of geological studies in Ireland. *Geol. Soc. Lond. Spec. Publ.* **2007**, *281*, 137–153. [CrossRef]
26. Feurer, D.; Vinatier, F. Joining multi-epoch archival aerial images in a single SfM block allows 3-D change detection with almost exclusively image information. *ISPRS J. Photogramm. Remote Sens.* **2018**, *146*, 495–506. [CrossRef]
27. Lowe, D.G. Distinctive image features from scale-invariant keypoints. *Int. J. Comput. Vis.* **2004**, *60*, 91–110. [CrossRef]

28. Lukyanenko, R.; Parsons, J.; Wiersma, Y.F. Emerging problems of data quality in citizen science: Editorial. *Biol. Conserv.* **2016**, *30*, 447–449. [CrossRef]
29. Kosmala, M.; Wiggins, A.; Swanson, A.; Simmons, B. Assessing data quality in citizen science. *Front. Ecol. Environ.* **2016**, *14*, 551–560. [CrossRef]
30. Balázs, B.; Mooney, P.; Nováková, E.; Bastin, L.; Jokar Arsanjani, J. Data Quality in Citizen Science. In *The Science of Citizen Science*, 1st ed.; Vohland, K., Land-Zandstra, A., Ceccaroni, L., Lemmens, R., Perelló, J., Ponti, M., Samson, R., Wagenknecht, K., Eds.; Springer International Publishing: Cham, Switzerland, 2021; pp. 139–157. [CrossRef]
31. Ratner, J.J.; Sury, J.J.; James, M.R.; Mather, T.A.; Pyle, D.M. Crowd-sourcing structure-from-motion data for terrain modelling in a real-world disaster scenario: A proof of concept. *Prog. Phys. Geogr. Earth Environ.* **2019**, *43*, 236–259. [CrossRef]
32. Miles, H.C.; Wilson, A.T.; Labrosse, F.; Tiddeman, B.; Griffiths, S.; Edwards, B.; Ritsos, P.D.; Mearman, J.W.; Möller, K.; Karl, R.; et al. Alternative Representations of 3D-Reconstructed Heritage Data. *J. Comput. Cult. Herit.* **2016**, *9*, 1–18. [CrossRef]
33. Kotovirta, V.; Toivanen, T.; Tergujeff, R.; Häme, T.; Molinier, M. Citizen Science for Earth Observation: Applications in environmental moitoring and disaster response. *Int. Arch. Photogramm. Remote Sens. Spat. Inf. Sci.* **2015**, *XL-7/W3*, 1221–1226. [CrossRef]
34. Scicchitano, G.; Scardino, G.; Tarascio, S.; Monaco, C.; Barracane, G.; Locuratolo, G.; Milella, M.; Piscitelli, A.; Mazza, G.; Mastronuzzi, G. The First Video Witness of Coastal Boulder Displacements Recorded during the Impact of Medicane "Zorbas" on Southeastern Sicily. *Water* **2020**, *12*, 1497. [CrossRef]
35. Guenzi, D.; Godone, D.; Allasia, P.; Fazio, N.L.; Perrotti, M.; Lollino, P. Brief communication: Monitoring a soft-rock coastal cliff using webcams and strain sensors. *Nat. Hazards Earth Syst. Sci.* **2022**, *22*, 207–212. [CrossRef]
36. Soloy, A.; Turki, I.; Lecoq, N.; Gutiérrez Barceló, Á.D.; Costa, S.; Laignel, B.; Bazin, B.; Soufflet, Y.; Le Louargant, L.; Maquaire, O. A fully automated method for monitoring the intertidal topography using Video Monitoring Systems. *Coast. Eng.* **2021**, *167*, 103894. [CrossRef]